On Finite Element Methods for 3D Time-Dependent Convection–Diffusion–Reaction Equations with Small Diffusion

Volker John and Ellen Schmeyer

Abstract The paper studies finite element methods for the simulation of time-dependent convection-diffusion-reaction equations with small diffusion: the SUPG method, a SOLD method and two types of FEM–FCT methods. The methods are assessed, in particular with respect to the size of the spurious oscillations in the computed solutions, at a 3D example with nonhomogeneous Dirichlet boundary conditions and homogeneous Neumann boundary conditions.

1 Introduction

The simulation of various applications requires the numerical solution of time-dependent convection–diffusion–reaction equations. Processes which involve a chemical reaction in a flow field are a typical example [5]. Such a reaction can be modeled with a coupled system of time-dependent nonlinear convection–diffusion–reaction equations for the concentrations of the reactants and the products.

Typically, the solution of these equations possesses layers. A numerical method for the simulation of these equations, whose results can be considered to be useful, should meet the following requirements:

- The layers should be correctly localized,
- Sharp layers (with respect to the used mesh size) should be computed,
- Spurious oscillations in the solution must not occur.

The third requirement means in particular that the computed solution should not have negative values if, for instance, the behavior of concentrations is simulated. A number of finite element methods have been developed for the simulation of convection–diffusion–reaction equations with small diffusion. One of the most popular ones is the Streamline Upwind Petrov–Galerkin (SUPG) method from [1, 2].

V. John (✉)
FR 6.1 – Mathematik, Universität des Saarlandes, Postfach 15 11 50, 66041 Saarbrücken, Germany,
E-mails: john@math.uni-sb.de, schmeyer@math.uni-sb.de

A.F. Hegarty et al. (eds.), *BAIL 2008 - Boundary and Interior Layers.*
Lecture Notes in Computational Science and Engineering,
DOI: 10.1007/978-3-642-00605-0,

This method leads to solutions with correctly located and sharp layers, however also with sometimes considerable spurious oscillations. To reduce these oscillations, a number of so-called Spurious Oscillations at Layers Diminishing (SOLD) schemes have been proposed, see the reviews [3,4]. SOLD schemes add additional, in general nonlinear, stabilization terms to the SUPG method. A completely different finite element approach for treating equations with small diffusion is used in Finite Element Method Flux–Corrected–Transport (FEM–FCT) schemes [8,10]. These methods do not modify the bilinear form but manipulate the matrix and the right-hand side of a Galerkin finite element method.

A first comparison of finite element methods for time-dependent convection-diffusion-reaction equations was presented in [6]. The numerical examples of [6] studied problems in 2D with homogeneous Dirichlet boundary conditions. The present paper extends the studies of [6] to 3D problems with inhomogeneous Dirichlet and homogeneous Neumann boundary conditions. This is a realistic situation in applications.

2 Finite Element Methods for Time-Dependent Convection–Diffusion–Reaction Equations

We consider a linear time-dependent convection–diffusion–reaction equation

$$u_t - \varepsilon \Delta u + \mathbf{b} \cdot \nabla u + cu = f \text{ in } (0,T] \times \Omega, \tag{1}$$

where $\varepsilon > 0$ is the diffusion coefficient, $\mathbf{b} \in L^\infty(0,T;(W^{1,\infty}(\Omega))^3)$ is the convection field, $c \in L^\infty(0,T;L^\infty(\Omega))$ is the non-negative reaction coefficient, $f \in L^2(0,T;L^2(\Omega))$ describes sources, $T > 0$ is the final time and $\Omega \subset \mathbb{R}^3$ is a bounded domain. This equation has to be equipped with an initial condition $u_0 = u(0,\mathbf{x})$ and with appropriate boundary conditions. Since the isothermal reaction considered in [5] leads to equations with non-negative reaction rates, we are particularly interested in the case $c(t,\mathbf{x}) \geq 0$ in $[0,T] \times \Omega$.

In the numerical studies, (1) is discretized in time with the Crank–Nicolson scheme using equidistant time steps Δt. This leads at the discrete time t_k to the equation

$$\begin{aligned} u_k &+ 0.5\Delta t\,(-\varepsilon \Delta u_k + \mathbf{b}_k \cdot \nabla u_k + c_k u_k) \\ &= u_{k-1} - 0.5\Delta t\,(-\varepsilon \Delta u_{k-1} + \mathbf{b}_{k-1} \cdot \nabla u_{k-1} + c_{k-1} u_{k-1}) \\ &\quad + 0.5\Delta t f_{k-1} + 0.5\Delta t f_k. \end{aligned} \tag{2}$$

Equation (2) can be considered as a steady-state convection–diffusion–reaction equation, with the diffusion, convection and reaction, respectively, given by

$$D = 0.5\Delta t \varepsilon, \quad \mathbf{C}_k = 0.5\Delta t \mathbf{b}_k, \quad R_k = 1 + 0.5\Delta t c_k.$$

The Galerkin finite element method for (2) reads as follows: Find $u_k^h \in V_{\text{ans}}^h$ such that

$$\begin{aligned}
&(u_k^h, v^h) + 0.5\Delta t \left((\varepsilon \nabla u_k^h, \nabla v^h) + (\mathbf{b}_k \cdot \nabla u_k^h + c_k u_k^h, v^h) \right) \\
&= (u_{k-1}^h, v^h) - 0.5\Delta t \left((\varepsilon \nabla u_{k-1}^h, \nabla v^h) + (\mathbf{b}_{k-1} \cdot \nabla u_{k-1}^h + c_{k-1} u_{k-1}^h, v^h) \right) \\
&\quad + 0.5\Delta t (f_{k-1}, v^h) + 0.5\Delta t (f_k, v^h)
\end{aligned} \tag{3}$$

for all $v^h \in V_{\text{test}}^h$, where V_{ans}^h and V_{test}^h are appropriate finite element spaces. Here, $(\cdot, \cdot)$ denotes the inner product in $L^2(\Omega)$.

The SUPG method adds a consistent diffusion term in streamline direction

$$\sum_{K \in \mathcal{T}^h} \tau_K \left(R^h(u_k^h), \mathbf{C}_k \cdot \nabla v^h \right)_K$$

to the left-hand side of (3), where $\mathcal{T}^h$ is the given triangulation of Ω, $\{\tau_K\}$ is a set of parameters depending on the mesh cells $\{K\}$ and $(\cdot, \cdot)_K$ is the inner product in $L^2(K)$. The residual $R^h(u_k^h)$ is defined by the difference of the left-hand side and the right-hand side of (2). Different proposals for the choice of the parameters $\{\tau_K\}$ can be found in the literature. In the numerical studies of [6], the choice from [7]

$$\tau_K = \min \left\{ \frac{h_K}{\Delta t \|\mathbf{b}_k\|_2}, \frac{1}{1 + 0.5\Delta t c_k}, \frac{2h_K^2}{\Delta t \varepsilon} \right\} \tag{4}$$

has been proven to be the best one. In (4), $\|\cdot\|_2$ denotes the Euclidean norm of a vector and h_K is an appropriate measure of the size of the mesh cell K. For time-dependent problems which are discretized with small time steps, the second term in (4) dominates and the actual choice h_K is of minor importance. In the computations presented below, the diameter of the mesh cell K was chosen. It is well known that numerical solutions which are computed with the SUPG method often possess non-negligible spurious oscillations at the layers.

SOLD methods try to reduce the spurious oscillations of the SUPG method by adding another stabilization term to this method. This stabilization term is in general nonlinear. There are several classes of SOLD methods, see [3, 4]. It was found in the numerical studies of [6] that the best results among the SOLD methods were obtained with a method that adds an anisotropic diffusion term

$$(\tilde{\varepsilon} \mathbb{C}_{\text{os},k} \nabla u_k^h, \nabla v^h) \quad \text{with} \quad \mathbb{C}_{\text{os},k} = \begin{cases} I - \dfrac{\mathbf{C}_k \otimes \mathbf{C}_k}{\|\mathbf{C}_k\|_2^2} & \text{if } \mathbf{C}_k \neq \mathbf{0}, \\ 0 & \text{else,} \end{cases}$$

and the parameter

$$\tilde{\varepsilon}|_K = \max \left\{ 0, C \frac{\operatorname{diam}(K) |R^h(u_k^h)|}{2\|\nabla u_k^h\|_2} - D \right\}, \tag{5}$$

where $\mathrm{diam}(K)$ is the diameter of a mesh cell K. This type of parameter was proposed in [7] and modified to the form (5) in [3]. The SOLD parameter (5) contains a free parameter C which has to be chosen by the user. In analogy to [6], this SOLD method will be called KLR02.

The last approaches which will be studied in our numerical tests are FEM–FCT schemes. They start with the algebraic equation corresponding to the Galerkin finite element method (3)

$$(M_C + 0.5\Delta t A_k)\underline{u}_k = (M_C - 0.5\Delta t A_{k-1})\underline{u}_{k-1} + 0.5\Delta t \underline{f}_{k-1} + 0.5\Delta t \underline{f}_k, \quad (6)$$

where $\{\varphi_i\}$ is the basis of the finite element space and $(M_C)_{ij} = (m_{ij}) = (\varphi_j, \varphi_i)$ is the consistent mass matrix. The matrix representation of the second term of the left-hand side of (3) is denoted by $(A_k)_{ij} = (a_{ij})$. Vectors are indicated by an underline. The first idea of FEM–FCT schemes is to manipulate (6) so that a stable but low order scheme is represented. To this end, define $L_k = A_k + D_k$ with

$$D_k = (d_{ij}), \quad d_{ij} = -\max\{0, a_{ij}, a_{ji}\} \text{ for } i \neq j, \; d_{ii} = -\sum_{j=1, j\neq i}^{N} d_{ij},$$

and $M_L = \mathrm{diag}(m_i)$ with $m_i = \sum_{j=1}^{N} m_{ij}$, where N is the number of degrees of freedom. M_L is called lumped mass matrix. The low order scheme reads

$$(M_L + 0.5\Delta t L_k)\underline{u}_k = (M_L - 0.5\Delta t L_{k-1})\underline{u}_{k-1} + 0.5\Delta t \underline{f}_{k-1} + 0.5\Delta t \underline{f}_k. \quad (7)$$

The second idea of FEM–FCT schemes is to modify the right-hand side of (7) in such a way that diffusion is removed where it is not needed but spurious oscillations are still suppressed

$$(M_L + 0.5\Delta t L_k)\underline{u}_k = (M_L - 0.5\Delta t L_{k-1})\underline{u}_{k-1} + 0.5\Delta t \underline{f}_{k-1} + 0.5\Delta t \underline{f}_k + \underline{f}^*(\underline{u}_k, \underline{u}_{k-1}). \quad (8)$$

The computation of the anti-diffusive flux vector $\underline{f}^*(\underline{u}_k, \underline{u}_{k-1})$ is somewhat involved and we refer to [6, 8–10] for details. Its computation relies on a predictor step which uses an explicit and stable low order scheme. Thus, a stability issue arises in FEM–FCT schemes which leads to the CFL-like condition $\Delta t < 2 \min_i m_i / l_{ii}$. This condition was fulfilled in the numerical tests presented in Sect. 3. We will consider a nonlinear approach for computing $\underline{f}^*(\underline{u}_k, \underline{u}_{k-1})$ [9, 10] and a linear approach [8] (in the form which is presented in [6]).

3 Numerical Studies

We consider a situation which has some typical features of a chemical reaction in applications. First, the domain is three dimensional, $\Omega = (0, 1)^3$. There is an inlet at $\{0\} \times (5/8, 6/8) \times (5/8, 6/8)$ and an outlet at $\{1\} \times (3/8, 4/8) \times (4/8, 5/8)$.

The convection is given by $\mathbf{b} = (1, -1/4, -1/8)^T$, which corresponds to the vector pointing from the center of the inlet to the center of the outlet. Thus, the convection will not be aligned to the mesh. The diffusion is given by $\varepsilon = 10^{-6}$ and the reaction by

$$c(\mathbf{x}) = \begin{cases} 1 \text{ if } \|\mathbf{x} - g\|_2 \leq 0.1, \\ 0 \text{ else,} \end{cases}$$

where g is the line through the center of the inlet and the center of the outlet. That means, a reaction takes place only where the solution (concentration) is expected to be transported. The inlet boundary condition is

$$u_{\text{in}}(t) = \begin{cases} \sin(\pi t/2) & \text{if } t \in [0, 1], \\ 1 & \text{if } t \in (1, 2], \\ \sin(\pi(t-1)/2) & \text{if } t \in (2, 3]. \end{cases}$$

At the outlet, homogeneous Neumann boundary conditions are prescribed. Apart from inlet and outlet, the solution should obey homogeneous Dirichlet conditions on the boundary. The right-hand side was set to be $f = 0$ in Ω for all times and the final time in our numerical studies was $T = 3$. The initial condition was set to be $u_0 = 0$. The orders of magnitude for diffusion, convection, reaction and concentration correspond to the situation of [5].

Results will be presented for the P_1 finite element on a tetrahedral mesh and the Q_1 finite element on a hexahedral mesh. The number of degrees of freedom on both meshes is 35 937, including Dirichlet nodes. The diameter of the mesh cells is about 0.054 for the hexahedral mesh and between 0.054 and 0.076 for the tetrahedral mesh. The Crank–Nicolson scheme was applied with $\Delta t = 0.001$.

From the construction of the problem, it is expected that the solution is transported from the inlet to the outlet with a little smearing due to the diffusion. It should take values in $[0, 1]$. The size of the spurious oscillations in the numerical schemes will be illustrated with the size of the undershoots $u^h_{\min}(t)$, see Fig. 1. The undershoots are particularly dangerous in applications since they represent non-physical situations, like negative concentrations. Figure 2 shows the distribution of

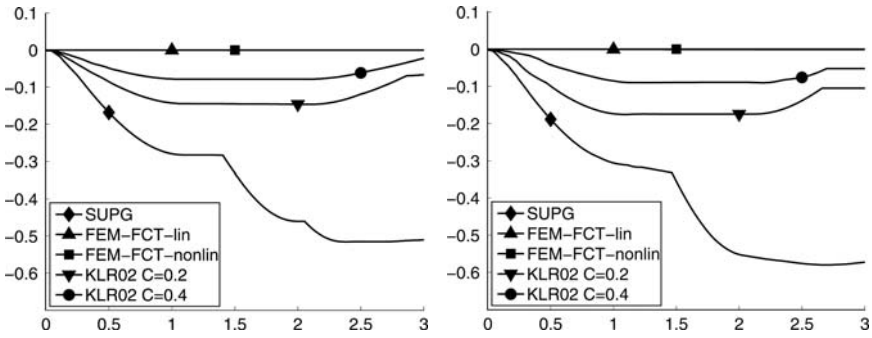

Fig. 1 Minimal value of the finite element solutions $u^h_{\min}(t)$, *left* Q_1, *right* P_1

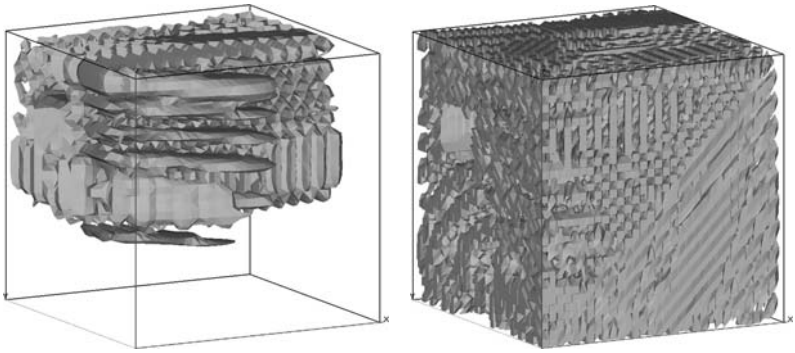

Fig. 2 Distribution of negative oscillations $u^h_{\min}(t) \leqslant 0.01$ for the SUPG method at $t = 2$, *left* Q_1, *right* P_1

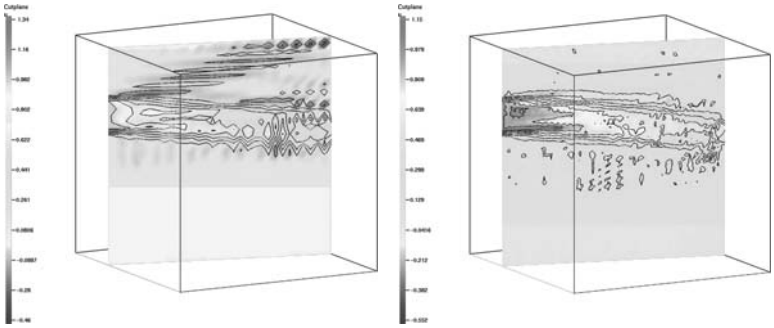

Fig. 3 Cut of the solution, SUPG method at $t = 2$, *left* Q_1, *right* P_1

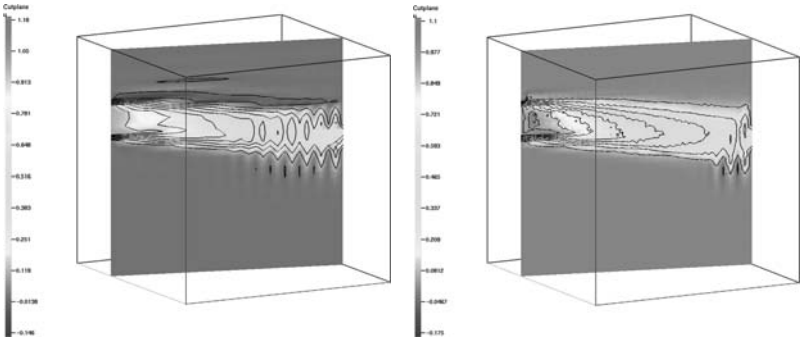

Fig. 4 Cut of the solution, SOLD method (5), $C = 0.2$ at $t = 2$, *left* Q_1, *right* P_1

the undershoots with $u^h_{\min}(t) \leqslant 0.01$ for the SUPG method at $t = 2$. Cut planes of the solutions at $t = 2$ are given in Figs. 3–7. These cut planes contain the centers of the inlet and the outlet and they are parallel to the z-axis. Note, some wiggles which can be seen in the contour lines might be due to the rather coarse meshes. For illustrating the spurious oscillations, a color bar is given for each cut plane.

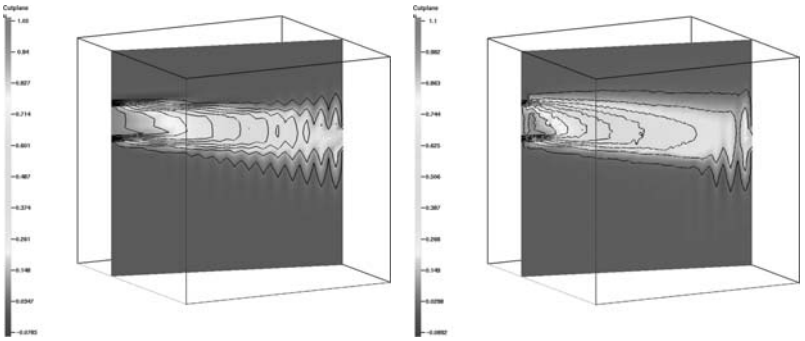

Fig. 5 Cut of the solution, SOLD method (5), $C = 0.4$ at $t = 2$, *left* Q_1, *right* P_1

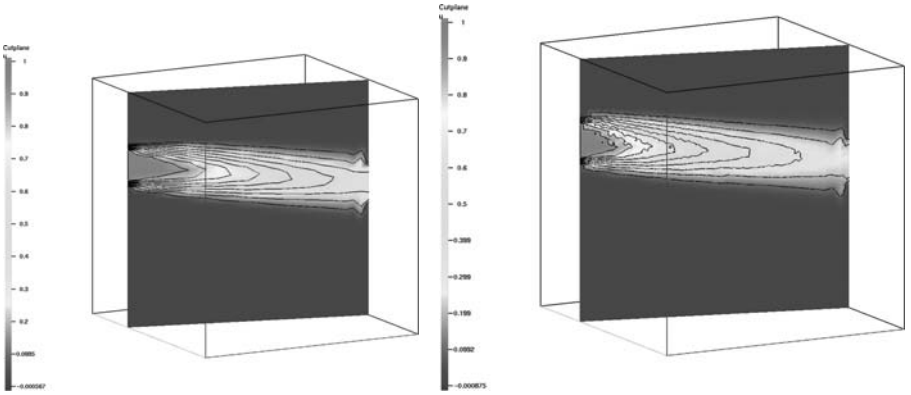

Fig. 6 Cut of the solution linear FEM–FCT method at $t = 2$, *left* Q_1, *right* P_1

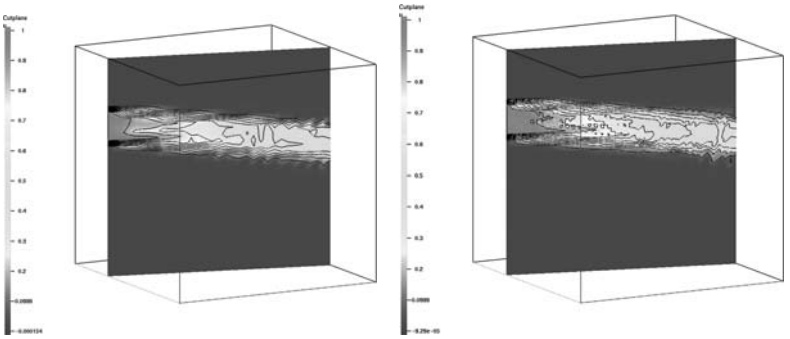

Fig. 7 Cut of the solution, nonlinear FEM–FCT method at $t = 2$, *left* Q_1, *right* P_1

The numerical results show the large amount of spurious oscillations in the solutions computed with the SUPG method. Figure 2 demonstrates that the solutions are globally polluted with spurious oscillations. The oscillations were considerably reduced and localized (not shown here) with the SOLD method KLR02. Increasing

Table 1 Computing times in seconds

Method	Q_1	P_1
SUPG	5,989	9,473
SOLD (5), $C = 0.2$	24,832	25,050
SOLD (5), $C = 0.4$	33,688	30,932
FEM–FCT linear	5,920	6,509
FEM–FCT nonlinear	9,768	10,398

the constant in (5) leads to a decrease of the spurious oscillations, Fig. 1. From the numerical studies of [3, 4] it is known that an increase of the constant in (5) results to somewhat more smearing of the solutions. However, this is rather tolerable in applications compared with spurious oscillations. The solutions obtained with the FEM–FCT methods are almost free of spurious oscillations. The smoother solutions of the linear FEM–FCT scheme, compared with the nonlinear FEM–FCT scheme, reflect that the linear scheme introduces more diffusion. This leads generally to a stronger smearing of the layers, see [6]. Altogether, the FEM–FCT schemes gave the best results in the numerical studies.

Computing times for the methods are given in Table 1. For solving the algebraic systems corresponding to the nonlinear schemes, the same fixed point iteration as described in [4, 6] was used. The iterations were stopped when the Euclidean norm of the residual was less than 10^{-8}. The computations were performed on a computer with Intel Xeon CPU with 2.66 GHz. It can be observed that the nonlinear schemes are considerably more expensive than the linear methods. For KLR02, the computing times increase with increasing size of the user-chosen parameter. All observations correspond to the results obtained in [6] for 2D problems.

4 Summary and Conclusions

The paper studied several finite element methods for solving time-dependent convection–diffusion–reaction equations in a 3D domain with inhomogeneous Dirichlet and homogeneous Neumann boundary conditions. The SUPG method led to solutions globally polluted with large spurious oscillations. These oscillations were reduced considerably with a SOLD method, but at the expense of much larger computing times. FEM–FCT methods led to almost oscillation-free solutions. From the aspects of solution quality and computing time, the linear FEM–FCT scheme seems to be, among the methods studied, the most appropriate method to be used in applications.

Acknowledgement The research of E. Schmeyer was supported by the Deutsche Forschungsgemeinschaft (DFG) by grant No. Jo 329/8–1 within the DFG priority program 1276 MetStröm: Multiple Scales in Fluid Mechanics and Meteorology.

References

1. A.N. Brooks and T.J.R. Hughes. Streamline upwind/Petrov-Galerkin formulations for convection dominated flows with particular emphasis on the incompressible Navier–Stokes equations. *Comput. Methods Appl. Mech. Eng.*, 32:199–259, 1982.
2. T.J.R. Hughes and A.N. Brooks. A multidimensional upwind scheme with no crosswind diffusion. In T.J.R. Hughes, editor, *Finite Element Methods for Convection Dominated Flows, AMD vol. 34*, pages 19–35. ASME, New York, 1979.
3. V. John and P. Knobloch. A comparison of spurious oscillations at layers diminishing (sold) methods for convection–diffusion equations: Part I – a review. *Comput. Methods Appl. Mech. Eng.*, 196:2197–2215, 2007.
4. V. John and P. Knobloch. A comparison of spurious oscillations at layers diminishing (sold) methods for convection–diffusion equations: Part II – analysis for P_1 and Q_1 finite elements. *Comput. Methods Appl. Mech. Eng.*, 197:1997–2014, 2008.
5. V. John, M. Roland, T. Mitkova, K. Sundmacher, L. Tobiska, and A. Voigt. Simulations of population balance systems with one internal coordinate using finite element methods. *Chem. Eng. Sci.*, 64:733–741, 2009.
6. V. John and E. Schmeyer. Stabilized finite element methods for time-dependent convection-diffusion–reaction equations. *Comput. Methods Appl. Mech. Eng.*, 198:475–494, 2008.
7. T. Knopp, G. Lube, and G. Rapin. Stabilized finite element methods with shock capturing for advection-diffusion problems. *Comput. Methods Appl. Mech. Eng.*, 191:2997–3013, 2002.
8. D. Kuzmin. Explicit and implicit FEM–FCT algorithms with flux linearization. Ergebnisberichte Angew. Math. 358, University of Dortmund, 2008. *J. Comput. Phys.*, 228:2517–2534, 2009.
9. D. Kuzmin and M. Möller. Algebraic flux correction I. Scalar conservation laws. In R. Löhner D. Kuzmin and S. Turek, editors, *Flux-corrected transport: Principles, algorithms and applications*, pages 155–206. Springer, Berlin, 2005.
10. D. Kuzmin, M. Möller, and S. Turek. High–resolution FEM–FCT schemes for multidimensional conservation laws. *Comput. Methods Appl. Mech. Eng.*, 193:4915–4946, 2004.